W/Fe co-sputtered layers for tungsten to steel joints

Nuclear Materials and Energy 35 (2023) 101421

Contents lists available at ScienceDirect

Nuclear Materials and Energy

journal homepage: www.elsevier.com/locate/nme

W/Fe co-sputtered layers for tungsten to steel joints

Valentina Casalegno [a,*], Sergio Perero [a], Vladimír Girman [d,e], Richard Sedlák [d], Alice Scarpellini [b], Daniel Dorow-Gerspach [c], Simon Heuer [c], Monica Ferraris [a]

[a] Politecnico di Torino, Dept. of Applied Science and Technology, c.so Duca degli Abruzzi 24, 10129 Torino, Italy
[b] Electron Microscopy Facility, Istituto Italiano di Tecnologia, Via Morego 30, 16163 Genova, Italy
[c] Forschungszentrum Jülich, Jülich 52425, Germany
[d] Institute of Materials Research of SAS, Watsonova 47, 04001 Kosice, Slovakia
[e] Faculty of Science, Institute of Physics, Pavol Jozef Safarik University in Kosice, Park Angelinum 9, 04001 Kosice, Slovakia

ARTICLE INFO

Keywords:
W/steel joints
Sputtering
Nuclear fusion

ABSTRACT

This work reports about preparation of W/Fe co-sputtered layers between tungsten and steel in order to ease their coefficient of thermal expansion mismatch.

Iron and tungsten have been gradually co-sputtered on W tiles with real time deposition parameters changing to obtain a graded interlayer: SEM, EDS, XPS, HR-TEM have been used to characterize the W/Fe co-sputtered layer.

W tiles co-sputtered with the W/Fe layers have been hot pressed to steel tiles: morphology and mechanical strength have been investigated for joints with and without W/Fe co-sputtered layer.

Lap-shear tests in compression at room temperature have been made on hot pressed W/steel joints with and without W/Fe co-sputtered layer, showing a different behaviour.

High flux test on joints with and without W/Fe co-sputtered layer are reported and discussed. The mechanical test results of manufactured joints are in good accordance with high heat flux test results, showing that the behaviour of hot-pressed joints with W/Fe co-sputtered layer was slightly worse if compared to joints without co-sputtered layer at the interface.

1. Introduction

For the first wall (FW) of the future fusion reactor, DEMO, tungsten and steel are considered prime materials. In particular, tungsten has been proposed as plasma facing material for both the divertor and the FW, while stainless steel will be used as structural material for the helium-cooled divertor.

Since the field lines and thus plasma impact on it in a direct manner, the divertor is the most heavily loaded component of a nuclear fusion reactor. Due to the high thermal load and severe plasma- and neutron-induced damage, divertor is expected to be manufactured of tungsten.

Several approaches have been proposed for manufacturing of the DEMO FW: all concepts combine the manufacturing of the inner structure using reduced activation ferritic-martensitic steel (RAFM steel) and protecting it on the plasma-facing side with a tungsten layer.

Several approaches to join W to steel are reported in [1], where different joining processes are listed and described (such as: direct solid state bonding, solid state bonding with discrete interlayers, brazing with and without additional layers, plasma spraying of discrete tungsten layers on steel, use of FGM tungsten/steel interlayers).

DEMO is the European Demonstration Power Plant, a future fusion energy facility that requires self-sufficiency in terms of tritium fuel [2,3]. The plasma in the reactor is surrounded by tritium breeding modules which are covered by the FW. The First Wall consists of plates of reduced-activation ferritic martensitic steel and contains cooling channels connected to a helium cycle for heat transfer and energy harvesting FW will be subjected to cyclic thermal load and bombardment by high-energy particles coming from plasma. As a consequence, a W protective coating is required for the FW of DEMO [1] and a sound joint between tungsten and steel is required.

Unfortunately, it is hard to achieve a direct connection between tungsten and steel because of the differences between their thermo-mechanical properties, which cause high stresses. Several techniques to solve this issue have been studied; ref. [1,4] report on the joining solutions proposed in literature.

Nowadays, brazing and diffusion bonding are the techniques being

* Corresponding author.
E-mail address: valentina.casalegno@polito.it (V. Casalegno).

https://doi.org/10.1016/j.nme.2023.101421
Received 16 January 2023; Received in revised form 26 February 2023; Accepted 17 March 2023
Available online 21 March 2023

considered to obtain W/steel joints. Brazing can be carried out by using brazing alloys foils or powders, in controlled atmosphere or in vacuum; most of the brazing alloys contain Cu, V, Ge or Ni [4–9].

Diffusion bonding can be carried out by hot isostatic pressing or by spark plasma sintering [10–12].

All the reported approaches to create strong W/steel joints are based on one or more of the following strategies: (a) choice of an interlayer with a thermal expansion coefficient (CTE) between W and steel to reduce the stress at the interface, (b) using a ductile interlayer which can deform and absorb the occurring strain difference, (c) joining processes at low temperatures (about 700 °C), (d) intermediate layer to create diffusion barrier and preventing the formation of brittle intermetallics at the W/steel interface [1].

As a consequence of what discussed above, the direct joining of tungsten and RAFM steel (i.e. Eurofer 97 in this work, referred to as steel from now on in the main content) is usually done by diffusion bonding, because this procedure requires the lowest possible welding temperatures.

However, despite relatively low temperature involved, the different CTE of the two materials (12×10^{-6} K^{-1} for steel and 4.4×10^{-6} K^{-1} for tungsten) causes the formation of excessive stresses during cooling from joining temperature to room temperature, which may generate a failure of the joint directly after manufacturing.

Additionally, further thermally induced stresses resulting from the pulsed operation of DEMO causes fatigue and may result in a premature failure of the joint.

It is widely believed that a metallic interlayer is necessary for the reduction of the high residual stress in the joined region; it is also required for the joint to sustain thermal cycle loadings between the operating temperature and room temperature [13].

Compared to directly joined W/steel components, the joint quality is assumed to increase because diffusion bonding now occurs between the Fe-rich last layer of the functionally graded material (FGM) and steel, instead of a direct bond between tungsten and steel.

Moreover, tungsten has a high creep strength at diffusion bonding temperature and it is considered inert in the formation of a joint, only the steel part contributing to the diffusion bonding [11].

Additionally, a diffusion bonding between the Fe-rich last layer of an FGM and steel, may need an even lower diffusion bonding temperature, with lower thermally induced stresses to the whole component.

Another benefit of the FGM is that stress peaks may be levelled because the CTE of tungsten and steel are gradually converged across the FGM layer. While this stress peak levelling should require layers in the range of millimetres, as predicted by numerical analyses in ref. [14], thin layers in the range of micrometres may improve the joint quality and can be produced by PVD (i.e. sputtering, in this work).

Finally, thin sputtered layers between bulk W and steel do not impede the heat removal from the hot plasma-side to the cooling channel compared to millimetre thick interlayers, thus reducing the temperatures in the whole component.

The sputtering is a promising technology for the deposition of homogeneous and high thermal conductivity layers and an be easily tailored in order to manufacture graded interlayers for joining tungsten to steel in plasma facing fusion components. The main advantage of sputtered layers is their negligible porosity, if compared to the intrinsic porosity and consequent relatively lower thermal conductivity of plasma sprayed layers [15–18].

In this work we investigate the potential of co-sputtered W/Fe layers on the W/steel joints for the first wall of DEMO.

2. Material and methods

W and steel (Eurofer 97) tiles of 12 mm × 12 mm × 4 mm and 16 mm × 16 mm × 3 mm were supplied by Forschungszentrum Jülich, Germany [19].

Pieces of W and steel were cut by electro discharge machining (EDM). After EDM, the top surface of the samples was removed by grinding and subsequent polishing (6, 3, 1 μm diamond suspension, followed by oxide polishing suspension (0.25 μm)). All samples were cleaned with acetone and isopropyl alcohol.

The W/Fe co-sputtered layers have been done by a customized Kenosistec™ sputtering equipment (IIT-Genova, Italy) equipped with four circular three inch diameter cathodes that can be powered up with direct current (DC), radiofrequency (RF) and pulsed DC. One cathode is designed for magnetic materials. The selected deposition atmosphere was Ar to avoid on-fly reactions and to reach the maximum deposition rate. The deposition pressure was dynamically controlled by a motorized and computer-controlled throttle valve and a gas regulator that allow to fine tuning of gas flowing and pressure in a wide range of values during deposition. The RF generators can power the cathodes up to 300 W, while the DC one can reach 500 W. Moreover, the DC generator can be used as Pulsed DC generator with a maximum frequency of 100 kHz. The iron was deposited using a DC pulsed magnetron cathode with a 100 Hz of reverse frequency and 3 μs of pulsing. The tungsten was deposited using a magnetron cathode, powered by a DC pulsed generator.

The W substrate has been heated up during deposition up to 450 °C and plasma etched before deposition to increase adhesion of the deposited layers.

A conventional hot press (by PVA TePla) was utilized to join W to steel tiles with and without co-sputtered layer: it features a high-vacuum furnace with Mo heaters and two titanium-zirconium-molybdenum (TZM) alloy press plates (300 mm × 300 mm × 100 mm). Alumina plates with a thin layer of boron nitride were used to prevent sticking of the metal pieces to the Mo TZM plates. A pressure sensitive foil was placed in between the steel and W piece and at a force of 9 kN, equalling a nominal pressure of 35 MPa, the homogeneity of the applied pressure was checked. When the color distribution was satisfying, the W piece was directly placed on the steel piece and 35 MPa were applied.

Then the chamber is evacuated to a pressure in the range of 10^{-4} to 10^{-3} Pa and heated to 650 °C in one hour (~11 °C/min). After a holding time of one hour to remove adsorbates and homogenize the temperature distribution, the temperature was increased to 800 °C in 50 min (3 °C/min). Having reached 800 °C, the uniaxial force is increased to 17,9 kN (70 MPa). After a holding time of two hours, the uniaxial force is reduced to 9 kN (35 MPa) and the passive cooling in high vacuum took about one day. This diffusion bonding parameters are based on a previous optimization study of the homologous joining of P92, a commercial steel similar to steel used in this work.

High Resolution SEM with Secondary Electron (SEI) and Backscattered Electron Imaging (RBEIJEOL JSM 7500FA), equipped with a cold FEG, operating at 10 kV acceleration voltage), EDS measurements and maps (Oxford X-Max 80 system with a Silicon Drift Detector with 80 mm^2 effective area of detecting device), XPS (XPS-Phi 5000 Versa Probe) and profilometry (Bruker Dektak Stilus™) were used to characterize the W/Fe co-sputtered layers. Characterization has been made on W/Fe co-sputtered layer deposited on silicon wafers (for analysis purpose only). Joined areas and interfaces have been analyzed as well, after cross-sectioning of the joints.

Transmission electron microscopy (TEM) observations were carried out using a JEOL 2100F UHR microscope equipped with Schottky FEG source powered by 200 kV. The observations were performed in scanning/transmission mode employing bright field detector (STEM BF). The EDS system (Oxford Instruments X-Max 80 SDD) was used for analysis and mapping of chemical composition. The samples were prepared by mechanical grinding and polishing. The final step was dimpling and ion milling (Gatan 691 PIPS). Before TEM observation the sample was cleaned in Plasma Cleaner (Fischione M1020) in order to ensure the residual-free surfaces of prepared foil. In particular, X-ray photoelectron spectroscopy was performed on the top of the sputtered layers, in order to perform more in-depth compositional analysis, for evaluating the elements that constitutes the first atomic layers and their bond state. In order to calibrate the binding energy scale, the carbon C1s (C–C) binding energy was set up at 284.5 eV.

The mechanical strength of the joined W/steel samples was measured using a single lap offset shear test at room temperature. The W and steel were joined to have a bonding surface of 8x16 mm^2, half overlapping of samples area. The load was applied by moving the cross-head at a speed of 0.5 mm/min, using a single lap offset (SLO) test under compression (equipment: universal testing machine SINTEC D/10), according to a method adapted from the ASTM D905-08 standard [20] and described in ref. [21].

The maximum force was recorded and the apparent shear strength was calculated by dividing the maximum force by the joined for SLO. The fracture surfaces were examined to determine fracture path and propagation by SEM.

To test the joints, cyclic high heat flux tests were performed using the electron beam facility JUDITH 2 [22]. Three stacks with and three without a sputtered interlayer were soldered on a copper cooling structure, allowing to verify the applied heat load via water calorimetry. The water-cooling conditions were 80 °C, 4.5 m/s flow speed at 2 MPa. After checking the proper alignment of the developed beam path at low intensity (about 0.3 MW/m^2), 200 cycles (30 s on / 30 s off) at power levels of 1, 2, 3, 4 MW/m^2 were applied. A thermography system of type ImageIR® 8380 from InfraTec GmbH monitors surface temperatures with a 640 × 512 pixel detector using a wavelength range of 2–5.7 µm was utilized. A tungsten emissivity curve from InfraTec was used to calculate the absolute temperature values. However, it should be noted that the emissivity value of a specific sample can differ substantially thus the absolute values should be seen as a rough estimation. The focus is on detecting changes and differences between the samples. The failure of a joint was declared, if the average surface temperature of a tile overcome roughly 2000 °C or even didn't reach a steady state during the loading phase. Also, a large inhomogeneity of the surface temperature due to partly broken joint was defined as failure. A drastic increase of the cooling time of the average temperature, after switching off the beam, accompanied such a failure. In some cases, the W tile became totally loose and had to be removed. The developed test procedure allows to exclude any failed sample from the beam path and to continue the test on the remaining ones.

3. Results

Twelve W tiles have been coated by W/Fe co-sputtered layers as sketched in Fig. 1, starting with 100 % W and zero Fe, followed by a gradual Fe increase until a 100% Fe and no W, deposited continuously, i.e. without interrupting the deposition, in order to obtain a continuously layer on W, as follows:

100% W; 80% W – 20% Fe; 60% W – 40% Fe; 50% W – 50% Fe; 40% W – 60% Fe; 20% W – 80% Fe; 100% Fe.

In order to achieve the composition previously described, long deposition time is required and higher power cannot be applied due to the magnetic effect of target materials. Several experimental trials have been carried out, but, in order to increase deposition rates and reduce deposition time, higher power and only a few layers were deposited. Pressure and total deposition time were fixed, and only power on cathodes was modified as reported in Table 1. Argon (Ar) was used as carrier gas to avoid oxidization and reactions during depositions.

W/Fe layers co-sputtered at 150,100 and 60 W DC-pulsed on Fe and 20, 30 and 50 W DC on W for 2 h to have three compositional zones only, with calculated atomic ratio between iron and tungsten of 30% tungsten – 70% iron, 50% tungsten – 50% iron, 70% tungsten – 30% iron, have been observed by cleaving the silicon used as a substrate to measure their thickness by profilometry, in triplicate, for each sample. The average total thickness of the W/Fe co-sputtered layers was about

Table 1
Deposition parameters, pressure, power and calculated atomic ratio.

LAYER	POWER on iron (W) -DC	POWER on tungsten (W) -DC
30% W-70% Fe	150	20
50% W-50% Fe	100	30
70% W-30% Fe	60	50

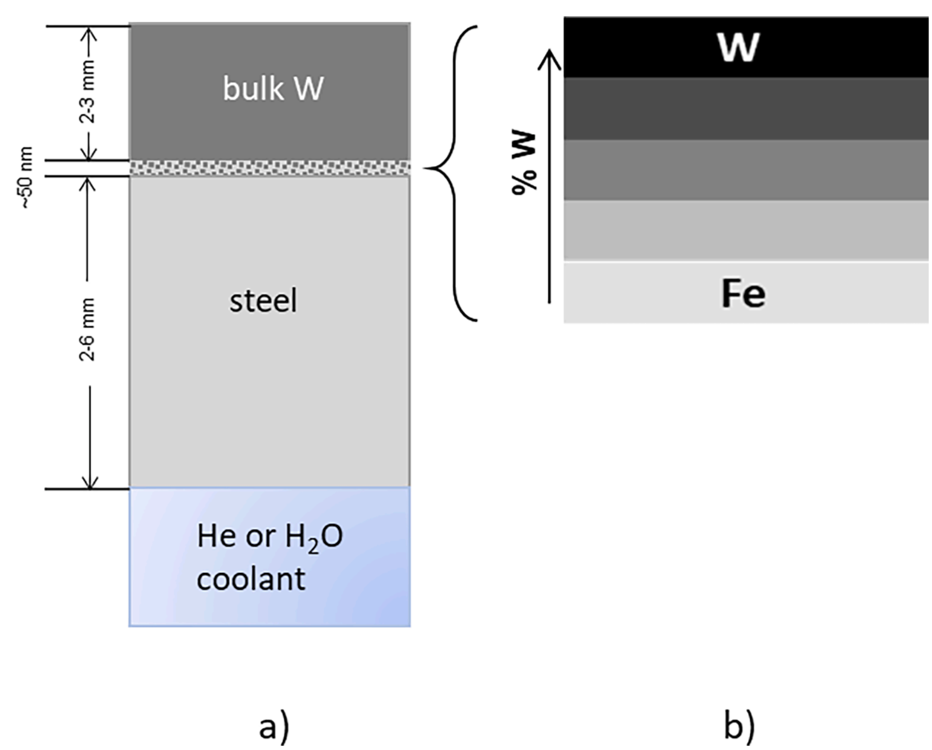

Fig. 1. Sketch of the W/Fe sputtered interlayer approach (a); a co-sputtered W/Fe layer (b) is deposited on W tiles, starting with 100 % W followed by a gradual Fe increase until a 100% Fe layer, which is then direct bonded to Eurofer by hot pressing.

45–50 nm.

High-resolution SEM with Secondary Electron detector has been used to observe the morphology of the W/Fe co-sputtered layers both in cross-section (Fig. 2 (a)) and top view (Fig. 2 (b)).

In order to distinguish the different composition amongst layers, high resolution SEM imaging has been acquired with a Retractable Backscattered Electron Detector (RBEI). The results of the layers' characterization are shown in Fig. 3. To be noticed, the contrast provided by the RBEI detector is based on atomic number differences: brighter contrast corresponds to a higher atomic number. Although compositional differences are visible, to some extent, it has to be pointed out that -even with a proper sample preparation-, it is difficult to precisely locate the end and start of each co-sputtered layer.

EDS compositional analysis has been done in zones 1 and 2 only, because zone 3 is too thin to obtain a reasonable compositional result; the compositional analysis (inset) gave measured values close to the calculated atomic ratio for two of the three zones. The zone 1 (yellow) in Fig. 3 has a thickness of about 17–20 nm, the zone 2 (blue) of about 20 nm and the zone 3 (green) of about 8–10 nm.

In order to fully investigate the surface composition of this W/Fe co-sputtered layer, and to investigate the last W-rich compositional zone, XPS measurements were done. XPS is specific to investigate the surface composition of a given materials, being able to test a few atomic layers on the sample surface: in this case, it gave 66 at % for W and 34 at % for Fe, (Fig. 4) consistent with composition expected with the selected sputtering process and parameters of Table 1.

The analyses reported in Figs. 2, 3 and 4 show that, even if the precise identification of zones with a different composition is not always possible due to the very low thickness of each zone, their structure is similar to what expected with the selected sputtering parameters.

According to these promising results, 12 tungsten tiles, deposited with W/Fe co-sputtered layer (as in Table 1) were joined with steel plates by hot pressing at 800 °C, 2 h, 70 MPa at FZJ as described before.

Fig. 5 shows a SEM image of a W/steel joint cross-section obtained by diffusion bonding, with W/Fe sputtered layers at the interface (not visible at this magnification).

In order to have a better characterization of the W/Fe co-sputtered layers inside the joint, STEM BF analyses have been done with different magnification in the joined region as shown in Fig. 6 (a,b).

The joint seam is about 40–50 nm and it has been highlighted by dotted lines. The joined seam shows some darker zones on both sides, characterized by different ratios of W/Fe. These regions were formed by diffusion of W/Fe co-deposited layers with steel and with W. EDS analyses reveals a continuous decreasing amount of Fe on the W side and *vice versa*.

Although several elements were detected (due to steel composition), on Fig. 6 only ratios of W and Fe (at %) are reported.

Fig. 7 shows the EDS mapping of the W/Fe co-sputtered layer inside the joint on two different magnifications, clearly demonstrating the W and Fe sides of the joint (Fig. 7 (a)) and, at higher magnification (Fig. 7 (b)) the co-existence of W and Fe in the co-sputtered layer.

Mechanical characterization of W/steel samples was carried out on manufactured samples.

In this work we proposed a Single Lap Offset (SLO) test in compression (Fig. 8), already used at Politecnico di Torino (Italy) for a quick comparison of several different joined samples [21,23]: it doesn't give a pure shear strength, but a useful comparison among different joined materials of the same size.

Eight hot pressed W/steel joints have been tested at room temperature, four with W/Fe co-sputtered layer and four without, for comparison purposes.

The W/steel joint samples to be mechanically tested have been produced by diffusion bonding with an offset of 2 mm (joined area 8x 16 mm^2); this step of sample preparation was a challenge. It was not possible cutting joints after joining process to obtain offset since it induces cracks in the samples.

Fig. 8 shows the Single Lap Offset test set up (inset) and the typical load/displacement curves after mechanical tests for hot pressed W/steel joints without (a) and with (b) W/Fe sputtered layer: both curves show a similar trend, typical of a brittle behavior of the joint; in (a), a step at about 6500 N can be possibly due to a crack formation in W.

Typical fracture surfaces after mechanical tests are shown in Fig. 9 for steel side (a,b) and W side (c, d); on the steel side (Fig. 9 (a) and (b)) two distinct regions can be observed: the darker area refer to steel surface, while the brighter area indicates residual W/Fe sputtered layer.

On the W side (Fig. 9 (c)and (d)), very few dark areas, corresponding to lighter elements (as Fe) can be detected, while white or mid-grey regions can be observed, corresponding to W and W-Fe respectively. Fig. 10 (a) shows a higher magnification of the W side of the joint after shear test: the white arrow indicates a crack, either present in the sample due to hot press process or developed during shear test. Plastic deformation of steel can be observed in Fig. 10 (b), which caused the stop of the mechanical test.

The limited number of samples does not allow a statistically relevant discussion, however, a summary of obtained results is in Fig. 11; it must be underlined that all the hot pressed 16 mm × 16 mm × 3 mm joints had the W tile cracked after hot pressing. The four 12 mm × 12 mm × 4 mm joints with W/Fe co-sputtered layer gave opposite results in two cases: fracture during positioning of the joint inside the testing fixtures in one case and plastic deformation of steel without fracture of the joint in another case.

To qualify a joining technique for a FW, a cyclic high flux test is very well suited and was done at FZJ. Six hot pressed W/steel joints, three with W/Fe co-sputtered layer and three without as reference were used.

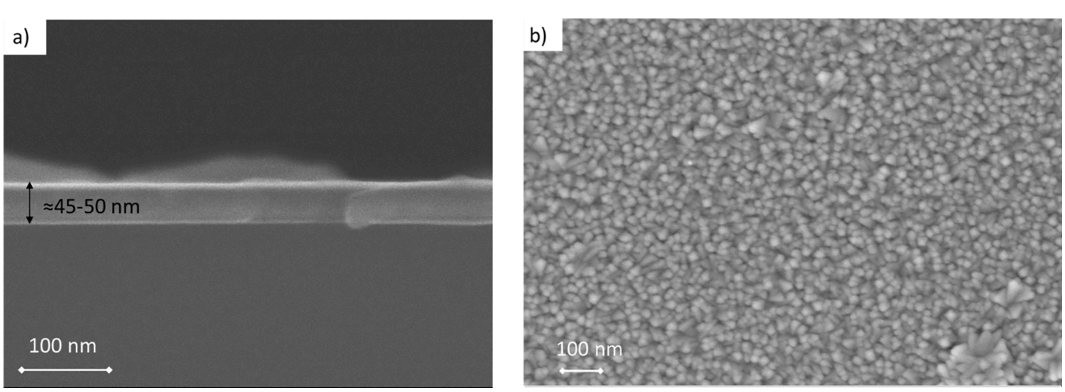

Fig. 2. High-resolution SEM with Secondary Electron detector (SEI) (JEOL JSM 7500FA, equipped with a cold FEG, operating at 10 kV acceleration voltage): Cross section (a) and top view (b) of the W/Fe co-sputtered layers deposited at 150 W pulsed- DC on iron and 20 W DC on tungsten, 100 W pulsed-DC on iron and 30 W DC on tungsten, and 60 W pulsed-DC on iron and 50 W DC on tungsten for 2 h *(sample deposited on silicon for analysis purpose only)*.

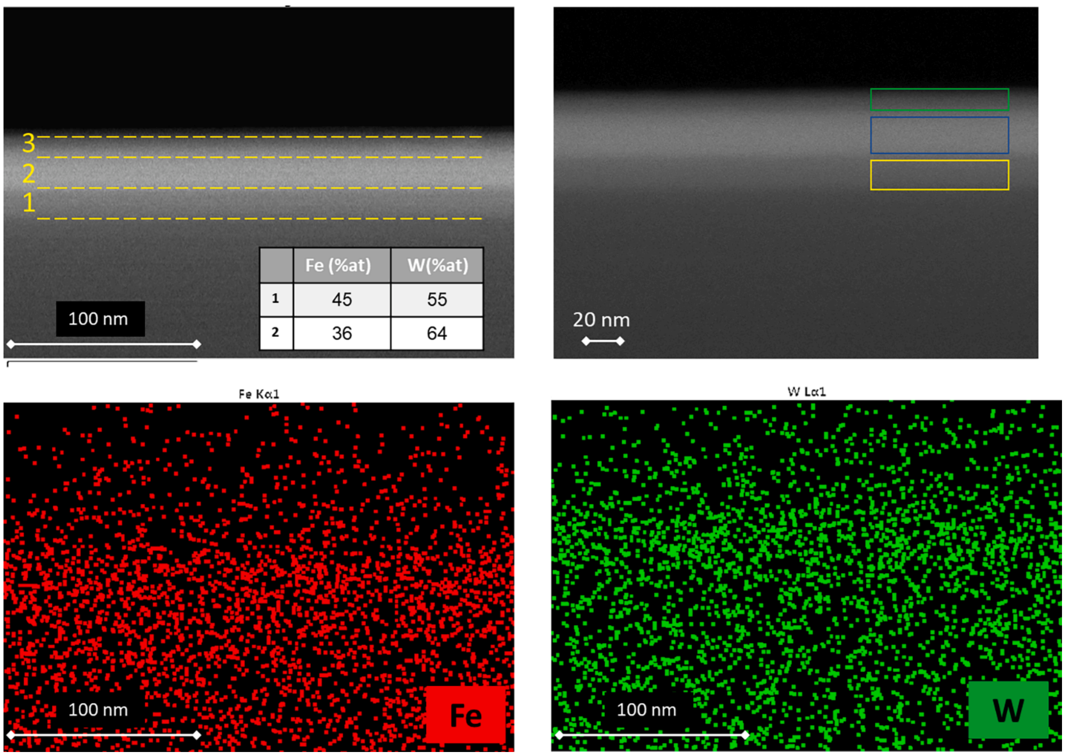

Fig. 3. High-resolution SEM and Retractable Backscattered Electron Imaging (RBEI) of the W/Fe sputtered layer (cross section); EDS compositional analysis in zones 1 and 2 (zone 3 is too thin to obtain a reasonable compositional result) *(sample deposited on silicon for analysis purpose only)*.

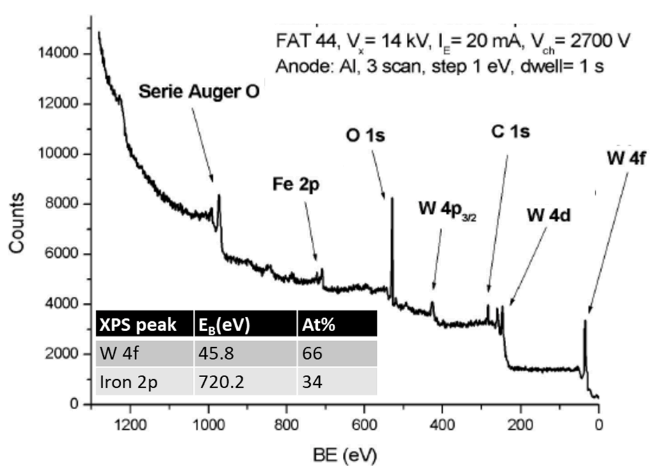

Fig. 4. XPS measurement W/Fe sputtered layer *(sample deposited on silicon for analysis purpose only)*.

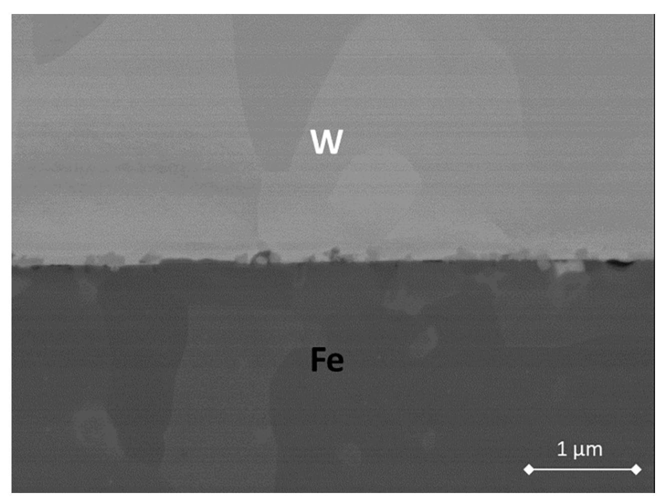

Fig. 5. SEM of W/Steel joint cross-section obtained by diffusion bonding, with W/Fe sputtered layers at the interface.

IR thermographs during high heat flux tests of samples with (left) sputtered FGM and (right) direct W/steel joint. The same tungsten emissivity calibration and the same scale was used for all thermographs. The images reported in Fig. 12 show the IR thermographs during high heat flux tests of samples with (left) sputtered FGM and (right) direct W-Fe joint.

3. Discussion

As shown in Fig. 1, W/Fe co-sputtered layers have been deposited on W tiles with gradual transition from 100% W to 100% Fe, decreasing W content and increasing Fe content.

In the frame of optimization of the joints, the number of co-sputtered layers and their compositions in terms of %W and %Fe were varied to assess favourable thickness of the FGM material at the interface between W and steel; a good compromise between obtained co-sputtered layers and deposition time/ power has been obtained with data reported in Table 1.

The W/Fe co-sputtered layers, as shown in Fig. 2, were homogeneous and crack free; no reaction layers have been detected at the interfaces between the co-sputtered layers and the substrates. No porosity or cracks were observed in the layers, both inside them and at the interfaces.

The co-sputtered layers are quite thin; the total thickness, as shown in Fig. 2, is about 50 nm and it was an initial attempt to investigate the feasibility of the co-sputtering process and to assess its morphological and thermo-mechanical performance. A thicker layer could lead to better minimization of CTE mismatch between W and steel, according to

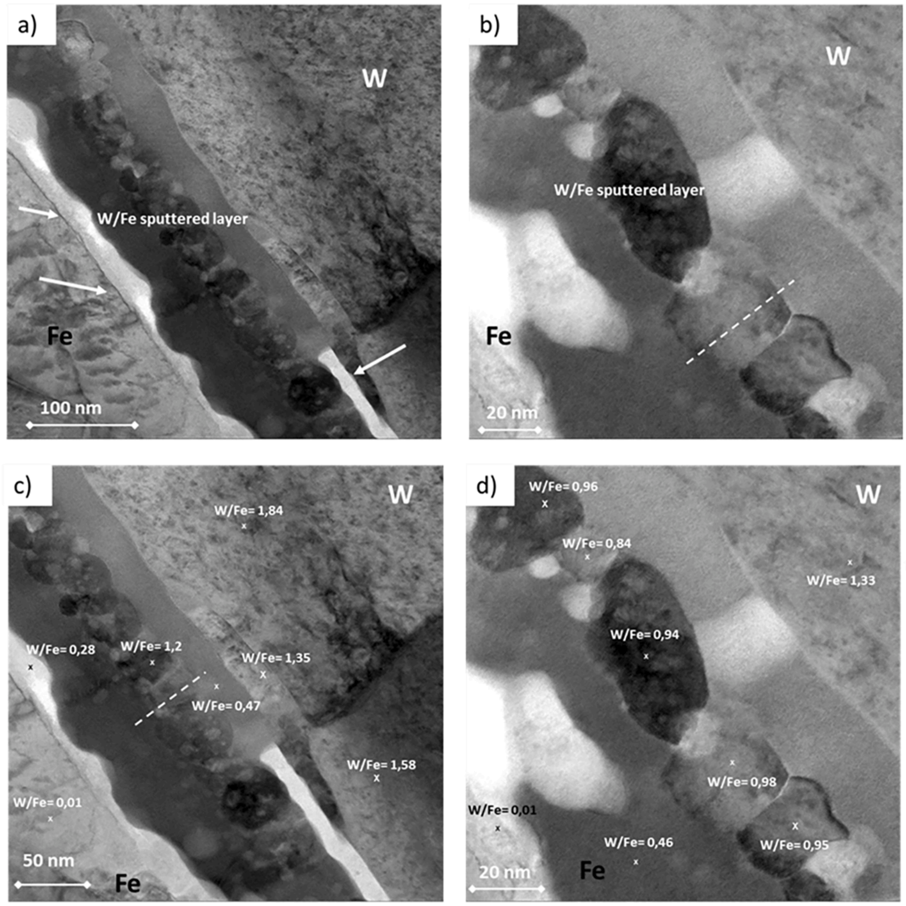

Fig. 6. STEM BF images of the joint with different magnification of the W/Fe sputtered layer in the joined region (arrows indicate nano-sized holes due to the ion milling process) (a,b); EDS point analysis: ratio between W and Fe (at%) is reported for each point (c,d).

what reported in [24]: the authors stated that a minimum FGM thickness of 1.2 mm is required for long-term coating performance. The formation of graded layers was confirmed by EDS analysis; each zone results from a co-sputtering of W and Fe. The EDS maps in Fig. 3 are still uncertain due to the very small area analysed: W seems to be more present on the upper zone, while Fe seems to be more abundant on the zone close to the silicon substrate, as expected. Having clarified this issue, the semi-quantitative EDS measurements indicate that the W/Fe ratio equals approximately to 80% for first layer (in contact with pure W) and 56% for the second layer. This is in good agreement with experimental parameters described in Table I for the manufacturing of co-sputtered layers. Consistent with this compositional analysis, XPS (Fig. 4) revealed a higher W content respect to Fe on the top surface layer.

The co-deposited sputtered layers have proven to be suitable for the manufacturing of tungsten to steel joints. The most significant result of the experimental activity was the manufacturing of sound joints obtained by direct bonding, using W/Fe co-sputtered layers at the interface, as observable in Fig. 5. Several studies have been reported in literature on graded structure between W and steel aimed at minimizing the stress at interface; for instance, [25] reported on the manufacturing by plasma spraying of graded interlayer made of several layers of W/steel-composites; the total thickness of the FGM layers is about 1.25 mm. The joint manufactured in the present work shows reduced thickness of graded layer at the interface, but this issue does not compromise the good metallurgical bond between tungsten and steel.

In this work, the W/Fe co-sputtered layers do not show porosity or intermetallics at the interface; the quality of bonding between the co-sputtered layer to substrates is good, as shown in Fig. 5. Moreover, no oxides have been detected on the steel surface, as it will be discussed in the following paragraph and it can be speculated that the thermal conductivity should not be significantly reduced since there is continuity between W and steel.

Moreover, implementing functionally graded interlayers in the W/steel joint can redistribute thermomechanical stresses at the interface and potentially extends the joint life-time.

A deeper analysis of the joint interface was carried out by STEM BF analysis. The cross-sectional micrograph of a complete joint reported in Fig. 6 shows magnified bonding interface; the structure is different from a conventional graded material, were layers of different composition are well visible. Especially, they are a phase mixture of tungsten particles/splats in a steel matrix [26]. In this case, the obtained material is 40–50 nm thick and shows a new and unknown structure, with different concentration of W and Fe uniformly changing from one side to the other one (arrows indicate nano-sized holes due to the ion milling process). The composition of the intermediate material manufactured by W/Fe sputtered layers was assessed by EDS analysis reported in Fig. 7; no localized formation of intermetallics was observed, but it was possible to observe (Fig. 7 (b)) the co-existence of W and Fe in the co-sputtered layer.

A temperature- and time-dependent precipitation of intermetallics will change material properties of FGM layers at W/steel joint during application.

The role of hot pressing in joints containing FGM interlayers must also be considered, since the high temperature and pressure and long dwelling time used to manufacture the joints can influence the joint morphology. The diffusion at the interface occurring during hot pressing process can smoothen the steps in composition of the different layers, thus providing an ideal FGM. In addition, diffusion at the co-sputtered

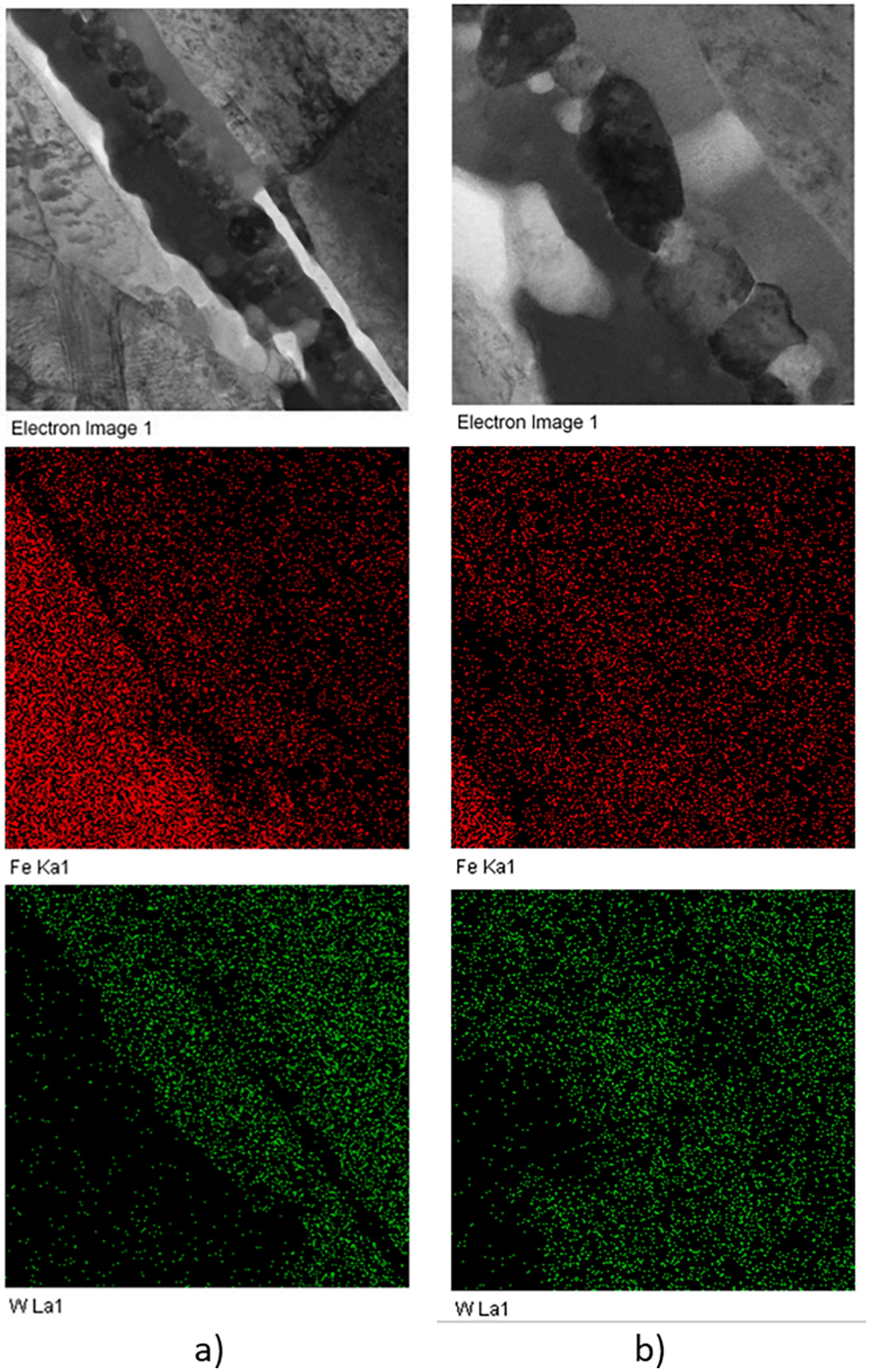

Fig. 7. EDS mapping of the joint with two different magnification of the W/Fe sputtered layer in the joined region, clearly showing the W and Fe sides (a) and the co-existence of W and Fe in the sputtered layer.

layers and at the W and steel interfaces can lead also to some kind of mixing.

The shear tests of W/steel joints brazed were performed to estimate the joint quality; mechanical behaviour was studied for both W/steel joints with W/Fe co-sputtered layers at the interface and W/steel joints without co-sputtered layer. Mechanical characterization of W/steel samples is not an easy task; several test configurations have been designed and reported in literature, varying the geometry of the test specimen, both for tensile and shear tests. [4,7,27–31].

In this work we used a Single Lap Offset (SLO) test in compression, as sketched in Fig. 8. This kind of test is not intended to measure the pure shear strength of the joints, but it can be used to make a comparison of the mechanical strength of joined materials of the same size.

The two measured values (15 and 21 MPa) are much lower than 61 and 88 MPa measured on hot pressed joints without W/Fe co-sputtered layer, (the other two gave cracks in the W tile). A statistical scattering is not unlikely because the brittle/sudden failure observed is often accompanied by strong scattering and a much larger number of shear-tested samples may help to understand. Moreover, the joining process and the single lap offset geometry are not perfect, possibly increasing scattering even more.

It demonstrates the favorable bonding of the two materials in both

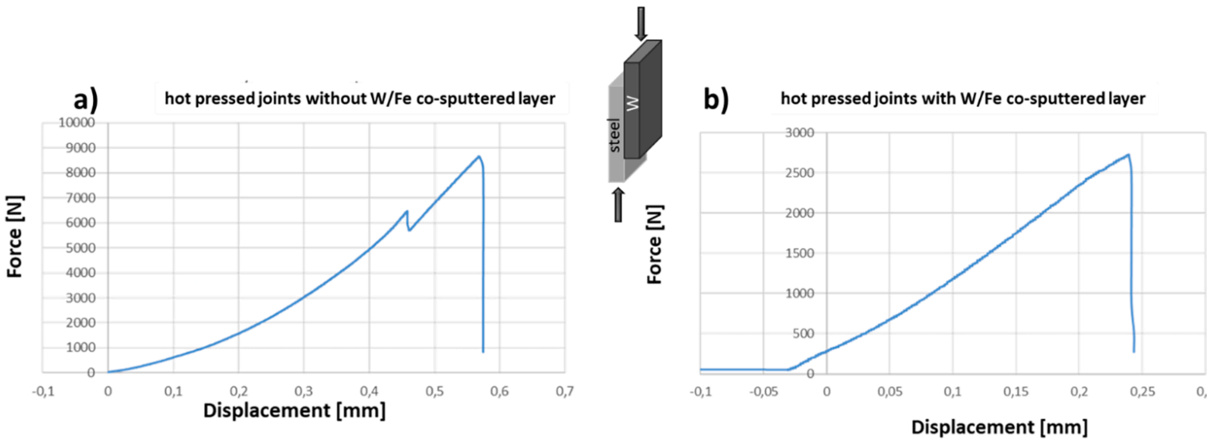

Fig. 8. Single Lap Offset test set up (inset), typical load/displacement curves after mechanical tests for hot pressed W/steel joints without (a) and with (b) W/Fe sputtered layer.

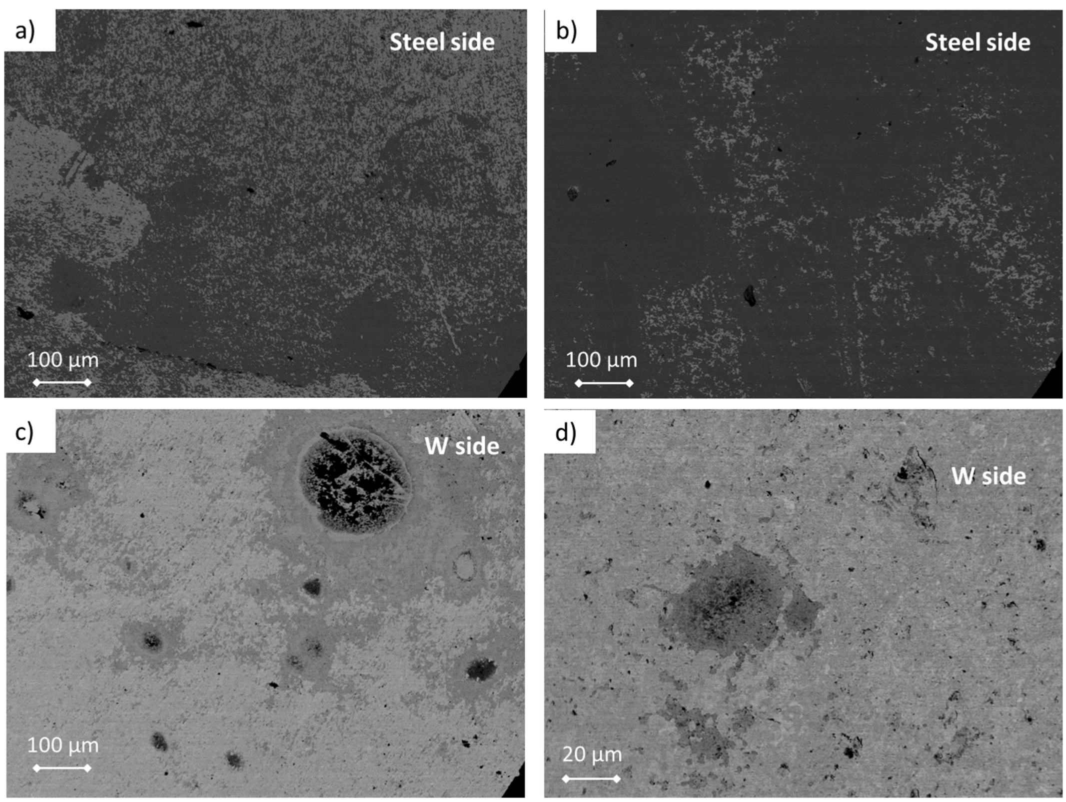

Fig. 9. SEM of fracture surfaces after mechanical tests for hot pressed W/steel joints with W/Fe sputtered layer: steel side (a,b); W side (c, d).

cases, even if it is not possible to compare the measured mechanical strength with that of samples obtained using other techniques, because of lack of mechanical test results in literature.

The failure surfaces (Fig. 9 (a-d) and Fig. 10) seem to suggest that failure occurred at the FGM layer or at the interface between W and FGM layer; additionally, elements contained in steel (Fe, Cr, detected by EDS, not reported here) and found on the W side together with W detected on the steel side are consistent with the diffusion process at the interface and confirm that at the diffusion bonding temperature the diffusion length of Fe in W is much smaller than the one of W in Fe.

To investigate the soundness of the joints, cyclic high heat flux tests were done and the results are presented in Fig. 12. The IR images reveal that already during alignment and the first cycle at 1 MW/m^2 one stack with W/Fe co-sputtered layer appeared significantly hotter. However, all six sustained 200 cycles at 1 MW/m^2 without any sign of further degradation. Nevertheless, increasing the heat load to 2 MW/m^2 led to an instantaneous failure of the joint of one sample with an interlayer and much hotter temperatures indicate damage also of the other two. Whereas the temperature increases of the directly joined references were within the estimated range due to the higher heat load. At cycle 77 also the last of the stacks with an FGM failed quite spontaneously, whereas no sign of degradation could be detected at the references (see Fig. 12 last row). They could even sustain the 3 MW/m^2 phase but all three failed during the first dozen cycles at 4 MW/m^2. According to FEM simulations, this translates to an interface temperature of roughly 550 °C above which fast deterioration of the direct W/steel joint of such small samples occurs.

The fact that the samples with the sputtered FGM failed at a much

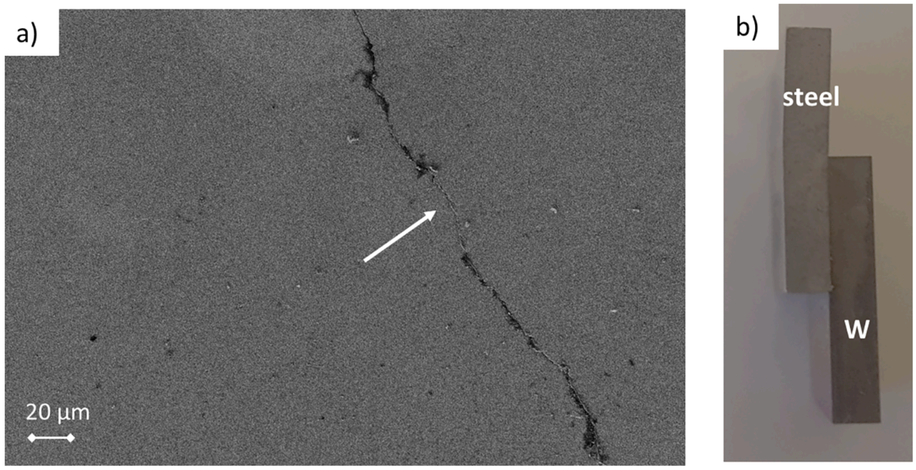

Fig. 10. SEM of fracture surfaces after mechanical tests for hot pressed W/steel joints with W/Fe sputtered layer: higher magnification of the W side (a); tested steel/W sample (b) showing bended steel and intact joint.

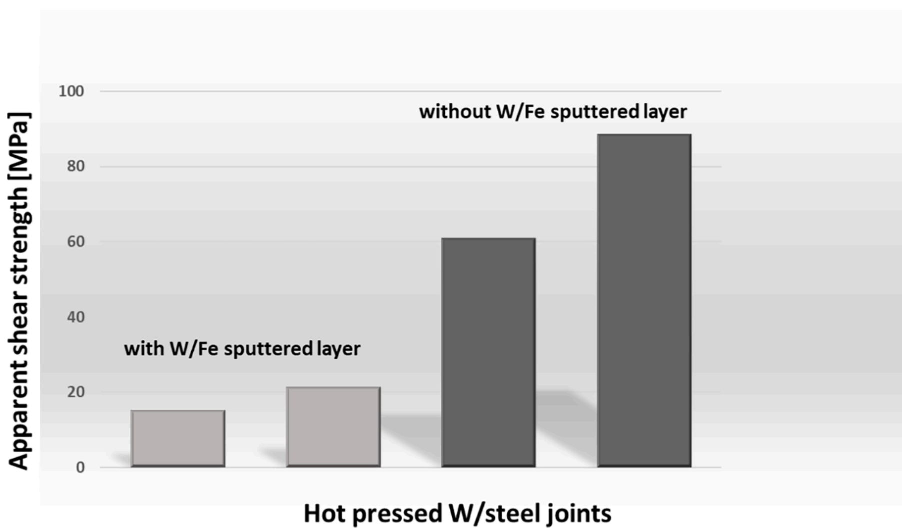

Fig. 11. Single Lap Offset results for hot pressed W/steel joints with (light grey bars) and without (dark grey bars) W/Fe sputtered layers.

lower heat flux than the reference is unfortunate but not utterly surprising, taking the results of the shear tests into account. As their stress bearing capability was indeed significantly lower (Figs. 8 and 11), they also fail at a lower interface temperature or power level, respectively.

The significance of the results obtained in this work lies in the use of W/Fe co-sputtered layers as suitable way to reduce CTE mismatch between tungsten and steel, forming a homogeneous layer at the joint interface containing W and F in graded percentage.

Furthermore, according to the Fe-W phase diagram the brittle intermetallic phase Fe7W6 forms already at the temperature of the cooling water of DEMO (~300 °C). Given the low thickness of the co-sputtered W/Fe layer, one possible issue could have been that the W/Fe co-sputtered layer is entirely transformed into intermetallics during hot pressing.

Since adding nickel to iron and tungsten is known to suppress the formation of the intermetallics, but in fusion, nickel is considered problematic due to its strong activation, given the high flexibility of magnetron sputtering and the very low amount of Ni potentially required in thin co-sputtered layers compared to thick sprayed layers, a next step could be the sputtering of a three-elements layer (Fe-Ni-W).

The three-elements system might be interesting to compare to the hot pressed W/steel joints, particularly after high flux tests.

4. Conclusions

It is evident that a suitable way to reduce the W/Fe CTE mismatch for joining of W to steel in application at high fluxes is still an open issue. The W/Fe co-sputtered layer discussed in this paper, far from being the envisaged solution, is nevertheless a novelty itself, being a homogeneous layer containing W and Fe in graded percentage.

It has been demonstrated that iron and tungsten can be gradually co-sputtered on W substrates to obtain graded interlayers able to minimize CTE mismatch, then subsequently joined to steel by hot pressing. Sputtering is an encouraging technology for the deposition of homogeneous, dense and high thermal conductivity layers to be used as graded interlayers for joining tungsten to steel in plasma facing fusion components.

Hot pressed W/steel joints have been successfully manufactured, some of them with W/Fe co-sputtered layer and others without, for comparison purposes. The mechanical test results for the two kinds of produced joints are in good accordance with HHF test results.

The performance of hot-pressed joints with W/Fe co-sputtered layer was slightly worse. Further work will be carried out to study more effective graded interlayers, able to maximize the stress concentration reduction at bonding interface.

In principle, the proposed joining solution can be a compromise

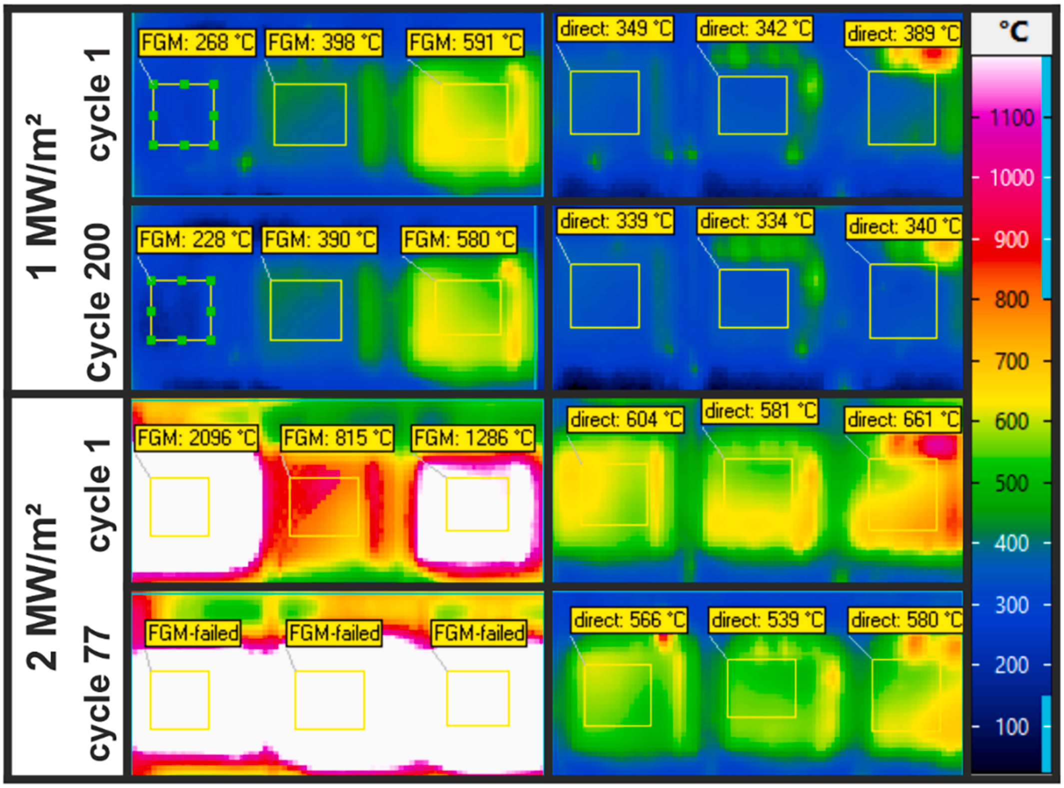

Fig. 12. IR thermographs during high heat flux tests of samples with (left) sputtered FGM and (right) direct W/steel joint. The same tungsten emissivity calibration and the same scale was used for all thermographs.

between direct W/steel joints (still critical in terms of mechanical strength) and brazed W/steel joints, still problematic in terms of elements diffusion during brazing process and increase of hardness in the seam area, thus leading to easy propagation of cracks at the interface. The W/Fe co-sputtered layers could demonstrate the potential of these layers for the use as stress reducing interlayer. Further investigation will be addressed also to determine the thermal conductivity at the interface of the W/Fe co-sputtered layers. The absence of porosity in these layers obtained by sputtering bodes well for increasing thermal conductivity.

The presented results have shown some potential limitations of these co-sputtered W/Fe layer and further work will be carried out to investigate some aspects, i. e by increasing their thickness. Moreover, in order to understand the influence of the hot pressing on joining, future work will be addressed to perform joining process at lower diffusion bonding temperature.

In conclusion, the W/Fe co-sputtered layer, away from being the intended solution, is nevertheless a novelty itself, being a homogeneous layer containing W and Fe in graded percentage obtained for the first time. It has been demonstrated that iron and tungsten can be gradually co-sputtered on W substrates to obtain graded interlayers, in principle able to minimize CTE mismatch, then subsequently joined to steel by hot pressing.

CRediT authorship contribution statement

Valentina Casalegno: Investigation, Analysis and Interpretation of data, Discussion of the results, Writing – review & editing. **Sergio Perero:** Experimental activity. **Vladimír Girman:** Experimental activity, Analysis and interpretation of data. **Richard Sedlák:** Experimental activity, Analysis and interpretation of data. **Alice Scarpellini:** Experimental activity, Validation of the results. **Daniel Dorow-Gerspach:** Methodology, Conceptualization, Analysis and interpretation of data, Review & editing. **Simon Heuer:** Analysis and interpretation of data. **Monica Ferraris:** Supervision, Funding acquisition, Writing – review & editing. All authors discussed the results and contributed to the final manuscript; all authors provided critical feedback and helped shape the research, analysis and manuscript preparation.

Declaration of Competing Interest

The authors declare that they have no known competing financial interests or personal relationships that could have appeared to influence the work reported in this paper.

Data availability

Data will be made available on request.

Acknowledgements

This work has been carried out within the framework of the EUROfusion Consortium, funded by the European Union via the Euratom Research and Training Programme (Grant Agreement No 101052200 — EUROfusion). Views and opinions expressed are however those of the author(s) only and do not necessarily reflect those of the European Union or the European Commission. Neither the European Union nor the European Commission can be held responsible for them.

References

[1] S. Heuer, J.W. Coenen, G. Pintsuk, J. Matějíček, M. Vilémováand, C. Linsmeier, Overview of challenges and developments in joining tungsten and steel for future fusion reactors, Phys. Scr. T171 014028 (2020), https://doi.org/10.1088/1402-4896/ab47a4.

[2] G. Federici, L. Boccaccini, F. Cismondi, M. Gasparotto, Y. Poitevin, I. Ricapito, An overview of the EU breeding blanket design strategy as an integral part of the DEMO design effort, Fus. Eng. Des. 141 (2019) 30–42, https://doi.org/10.1016/j.fusengdes.2019.01.141.

[3] A.J.H. Donné, G. Federici, A. Ibarra, J. Menard, F. Warmer, Magnetic Confinement Fusion—Development Facilities, Editor(s): Ehud Greenspan, Encyclopedia of Nuclear Energy, Elsevier (2021) 635-654, 10.1016/B978-0-12-819725-7.00103-3.

[4] D. Bachurina, V. Vorkel, A. Suchkov, J. Gurova, A. Ivannikov, M. Penyaz, I. Fedotov, O. Sevryukov, B. Kalin, Overview of the mechanical properties of tungsten/steel brazed joints for the demo fusion reactor, Metals (Basel) 11 (2021) 1–11, https://doi.org/10.3390/met11020209.

[5] D. Bachurina, A. Suchkov, J. Gurova, V. Kliucharev, V. Vorkel, M. Savelyev, P. Somov, O. Sevryukov, Brazing tungsten/tantalum/RAFM steel joint for DEMO by fully reduced activation brazing alloy 48Ti-48Zr-4Be, Metals 11 (2021) 1417, https://doi.org/10.3390/met11091417.

[6] D. Bachurina, A. Suchkov, Y. Gurova, O. Sevryukov, Investigation of a brazed joint EK-181/V/W obtained by Cu-Sn and Cu-Ti amorphous foil, IOP Conf. Ser. Mater. Sci. Eng. 1005 (2020), 012010, https://doi.org/10.1088/1757-899X/1005/1/012010.

[7] Y.Z. Ma, Q.S. Cai, W.S. Liu, S.H. Liu, Microstructure and mechanical properties of brazed tungsten/steel joint for divertor application, Mater. Sci. Forum 789 (2014) 384–390, https://doi.org/10.4028/www.scientific.net/MSF.789.384.

[8] J. de Prado, M. Sanchez, A. Urena, Improvements in W-Eurofer first wall brazed joint using alloyed powders fillers, Fus. Eng. Des. 124 (2017) 1082e1085, https://doi.org/10.1016/j.jnucmat.2020.152117.

[9] W. Zhu, J. Qiang, Y. Wang, J. Sun, J. Wang, Y. Lian, F. Feng, X. Liu, A Ti-Fe-Sn thin film assembly for joining tungsten and reduced activation ferritic-martensitic steels, Mater. Des. 125 (2017) 55–61, https://doi.org/10.1016/j.matdes.2017.03.060.

[10] W. Liu, X. Pang, Q. Cai, Y. Ma, W. Zhu, Fabrication of W/steel joint using hot isostatic pressing with Ti/Cu/Ti liquid forming interlayer, Fus. Eng. Des. 135 (2018) 59–64, https://doi.org/10.1016/j.fusengdes.2018.07.013.

[11] W.W. Basuki, J. Aktaa, Investigation of tungsten/STEEL diffusion bonding using Nb interlayer, Fus. Eng. Des. 86 (2011) 2585–2588, https://doi.org/10.1016/j.fusengdes.2011.03.017.

[12] C. Tan, C. Wang, S. Wang, G. Wang, L. Ji, Y. Tong, X.M. Duan, Investigation on 316L/316L-50W/W plate functionally graded materials fabricated by spark plasma sintering, Fus. Eng. Des. 125 (2017) 171–177, https://doi.org/10.1016/j.fusengdes.2017.08.001.

[13] M. Rieth, S.L. Dudarev, S.M. Gonzalez de Vicente, et al., Recent progress in research on tungsten materials for nuclear fusion applications in Europe, J. Nucl. Phys. Mater. Sci. Radiat. Appl. 432 (2013) 482–500, https://doi.org/10.1016/j.jnucmat.2012.08.018.

[14] S. Heuer, T. Weber, G. Pintsuk, J.W. Coenen, J. Matejicek, C. Linsmeier, Aiming at understanding thermo-mechanical loads in the first wall of DEMO: Stress–strain evolution in a Steel-tungsten test component featuring a functionally graded interlayer, Fus. Eng. Des. 135 (2018) 141–153, https://doi.org/10.1016/j.fusengdes.2018.07.011.

[15] F. Baptista, J. Silva, J. Porteiro, G. Míguez, Pinto, sputtering physical vapour deposition (PVD) coatings: a critical review on process improvement and market trend demands, Coatings 8 (2018) 402, https://doi.org/10.3390/coatings811040.

[16] J.G. Baptista, J. Silva, J.L. Porteiro, G. Míguez, L.F. Pinto, On the physical vapour deposition (PVD): evolution of magnetron sputtering processes for industrial applications A, Procedia Manuf. 17 (2018) 746–757.

[17] J. Neelesh, M. Sawant, S. Nikam, S. Jhavar, Metal Deposition: Plasma-Based Processes. 10.1081/E-EPLT-120053919. Encyclopedia of Plasma Technology (2016).

[18] Y. Yunzhi, K. Kyo-Han, O.L. Joo, A review on calcium phosphate coatings produced using a sputtering process—an alternative to plasma spraying, Biomaterials 26 (3) (2005) 327–337, https://doi.org/10.1016/j.biomaterials.2004.02.029.

[19] G. Pintsuk, G. Aiello, S. Dudarev, M. Gorley, J. Henry, M. Richou, M. Rieth, D. Terentyev, R. Vila, Materials for in-vessel components, Fus. Eng. Des. 174 (2022), 112994, https://doi.org/10.1016/j.fusengdes.2021.112994.

[20] ASTM D905-08; Standard Test Method for Strength Properties of Adhesive Bonds in Shear by Compression Loading. ASTM International: West Conshohocken, PA, USA, 2013.

[21] M. Suess, C. Wilhelmi, M. Salvo, V. Casalegno, P. Tatarko, M. Funke, Effect of pulsed laser irradiation on the SiC surface, Int. J. Appl. Ceram. Technol. 14 (3) (2017) 313–322.

[22] A. Schmidt, et al., High Heat Flux Testing of components for future fusion devices by means of the facility JUDITH 2, in: International Conference on High-Power Electron Beam Technology 2010 (EBEAM 2010), 1 Curran Associates, Inc., 2011, p. 571.

[23] M. Ferraris , M. Salvo , V. Casalegno , S. De La Pierre, L. Goglio, A. Benelli , Torsion test vs. other methods to obtain the shear strength of elastic-plastic adhesives, Appl. Sci. (Switzerland) 12(7) (2022) 3284 10.3390/app12073284.

[24] T. Grammes, T. Emmerich, D. Qu, O. Heinze, R. Vaßen, J. Aktaa, Functionally graded tungsten/EUROFER coating for DEMO first wall: from laboratory to industrial production, Fus. Eng. Des. 188 (2023), 113430.

[25] V. Ganesh, D. Dorow-Gerspach, S. Heuer, J. Matejicek, M. Vilemova, M. Bram, J. W. Coenen, M. Wirtz, G. Pintsuk, W. Theisen, C. Linsmeier, Manufacturing of W-steel joint using plasma sprayed graded W/steel-interlayer with current assisted diffusion bonding, Fus. Eng. Des. 172 (2021), 112896, https://doi.org/10.1016/j.fusengdes.2021.112896.

[26] V. Ganesh, L. Leich, D.D. Dorow-Gerspach, S. Heuer, J.W. Coenen, M. Wirtz, G. Pintsuk, F. Gormann, P. Lied, S. Baumgärtner, W. Theisen, C. Linsmeier, Manufacturing of W/steel composites using electro-discharge sintering process, Nucl. Mater. Energy 30 (2022), 101089, https://doi.org/10.1016/j.nme.2021.101089.

[27] W. Liu, Z. Wang, Y. Ma, Q. Cai, Investigation of tungsten/steel brazing using Ta and Cu interlayer, Fus. Eng. Des. 113 (113) (2016) 102–108, https://doi.org/10.1016/j.fusengdes.2016.11.004.

[28] Q. Cai, W. Liu, Y. Ma, Z. Wang, Diffusion brazing of tungsten and steel using Ti–Ni liquid phase forming interlayer, Fus. Eng. Des. 91 (2015), https://doi.org/10.1016/j.fusengdes.2014.12.029.

[29] W. Krauss, J. Lorenz, J. Konys, Performance of electro-plated and joined components for divertor application, Fus. Eng. Des. 88 (2013), https://doi.org/10.1016/j.fusengdes.2013.04.049.

[30] J. de Prado, M. Sanchez, A. Urena, Development of brazing process for W-STEEL joints using Cu-based fillers, Phys. Scr. 2016 (2016), 014022, https://doi.org/10.1088/0031-8949/T167/1/014022.

[31] J. de Prado, M. Sanchez, A. Urena, Evaluation of mechanically alloyed Cu-based powders as filler alloy for brazing tungsten to a reduced activation ferritic-martensitic steel, J. Nucl. Mater. 490 (2017) 188–196, https://doi.org/10.1016/j.jnucmat.2017.04.033.